Ethiopian Journal of Technical and Vocational Education and Training
ISSN: 3005-4362
Vol. 3 No. 1 January 2025

Effects of Coating Process Variables on the Thermal Conductivity of Cotton Knitted Fabrics Coated with Phase-Change Materials

Gurumurthy.B. Ramaiah[1*], Metusal Meja[2], Daniel Asfaw[3], Robel Legese[4], [5]Tolera A Negawo

[1,2,3,4,5] Department of TextileTechnology, Faculty of Textile and Apparel Fashion, Federal TVTI, P.O.Box: 190310, Addis Ababa, Ethiopia

[*]Corresponding Author: Gurumurthy.B. Email: Ramaiah voguru1@gmail.com

ABSTRACT

Phase change materials (PCMs) exhibit the ability to absorb, store, and release latent heat during phase transitions, making them ideal for enhancing thermal comfort and energy efficiency. In this study, PCM was applied to knitted cotton fabrics to develop thermo-regulated textile samples. Screen-printing techniques were employed for coating, with viscosity (56–62 centistokes) and number of strokes used as independent variables. The processing parameters were optimized using Response Surface Methodology (RSM) based on a Central Composite Design (CCD) in Design Expert Software. After coating, the samples were cured and dried in an oven. Thermal conductivity, the primary response variable, was measured using Lee's disk method. Fourier Transform Infrared (FTIR) spectroscopy data analyzed chemical functional groups in the coating material, and Differential Scanning Calorimetry (DSC) determined the melting point of the samples. Optimization results revealed the best thermal conductivity of 0.033 W/mK at a viscosity of approximately 61.4 centistokes and 5.9 strokes. For fabric processors seeking to enhance thermal performance without compromising fabric flexibility or other critical properties, this optimal condition provides a valuable guideline. Overall, the incorporation of PCM into textile structures through optimized screen-printing significantly improves thermal regulation, offering promising applications in smart and energy-efficient clothing.

KEYWORDS
Thermal Conductivity, Phase Change Material, Kulkote, Spray Coating, Screen printing, Viscosity

Introduction

The potential of phase change materials (PCMs), especially organic ones like polyethylene glycol (PEG) and benzene derivatives, to absorb, store, and release heat energy during physical state transitions—such as from solid to liquid—has drawn a lot of interest from the textile industry (Cenik, Oktay, Nallbani, & Kayaman-Apohan). Congruent fusion, high thermal stability, good heat storage capacity, and low corrosiveness are some of the essential properties that make these materials perfect for applications where temperature control is essential (Aksoy et al., 2024). Kulkote is a well-known commercial PCM product used in textiles that is applied using techniques including screen printing and spraying to enhance thermal performance. When PCMs are incorporated into textiles, clothing can reduce temperature swings, improving user comfort in a range of environmental settings. As a result, PCM-treated fabrics are seeing greater use in protective gear, sporting, medical apparel, bedding, and even aerospace applications where temperature control is essential (Chen et al., 2024).

PCMs are known to provide benefits in textiles, but there are still a number of issues that need to be addressed. A significant problem is that diverse fabric architectures and application techniques do not consistently provide long-term thermoregulation (Das et al.,2025). Furthermore, prolonged temperature regulation is anticipated from PCM-treated fabrics, whereas traditional cooling technologies frequently only offer short-term respite. Regarding the comparative evaluation of various fabric structures treated with PCM and the efficacy of different coating techniques, these issues draw attention to a gap in the literature (Ding et al., 2025).

Several research topics are intended to be addressed by this work. First, how well does Kulkote improve thermoregulation in cotton fabrics coated with PCM in different environmental settings? Second, how does the thermal behavior of fabrics treated with PCM depend on the textile architecture, such as knitted structures (El Majd et al., 2024)? Third, what are the differences between treated and untreated textiles in terms of their chemical characteristics as determined by Fourier Transform Infrared Spectroscopy (FTIR) (Kadam, Saini, Verma, Dubey, & Verma, 2024). Last but not least, which coating methods offer the most consistent and long-lasting PCM application for reliable thermal performance?

This study focuses on organic PCMs, specifically Kulkote, that are used on cotton textiles. Examining knitted textile fabric, the study concentrated on application methods such as screen printing. To characterize the treated textiles, laboratory techniques such as FTIR spectroscopy were employed. PCMs other than Kulkote and synthetic textiles were not used in the study (Li et al., 2025). By concentrating on these research problems, the study hopes to offer a thorough grasp of how PCMs act on knitted textile fabrics (Lang, Xiang, & Gao, 2024).

The development of PCM textile technology could be advantageous to sectors like healthcare, the military, outdoor recreation, and aerospace since efficient thermoregulation can improve comfort and safety in demanding settings (Omen et al, 2025). Additionally, this study may help improve the quality of sleep in consumer goods like mattresses and bedding, where it is critical to keep a constant temperature. This approach aids in directing the analysis by pointing out how various knitted cotton fabrics and treatment techniques impact PCMs' ability to maintain thermal balance (Raoux, 2009).

Materials and Methods

Materials

Materials used for this investigation included a piece of knitted fabric, 100% cotton single jersey fabric that has been bleached with hydrogen peroxide (H_2O_2). Kulkote was the phase change substance that was utilized; it came in a single bottle for application from the supplier (https://kulkote.com/). The instruments used to accomplish this work's goal included technical measurements that are made using equipment and accessories such as the Differential

Scanning Calorimeter (DSC), scanning electron microscopy (SEM), Fourier-transform infrared spectroscopy (FTIR), and others.

Sample development

Using the screen-printing technique, Kulkote phase change material was applied to knitted (single jersey, H_2O_2 bleached) fabrics. By modifying the printing parameters in accordance with the experimental design shown in Figure 1, the application procedure was completed. By using this method, the Kulkote material was applied on cloth with accuracy and consistency, allowing for a comparison of their post-treatment thermal performance (Shuai, Zhang, Hu, He, & Gong, 2025).

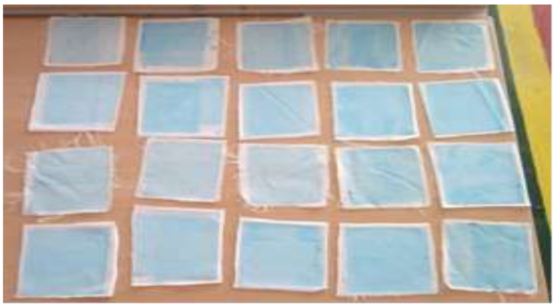

Figure 1. Samples developed by screen printing

Experimental design plan for screen printing

The independent variables used were the viscosity of the kulkote and the number of strokes in screen printing. The dependent (response) variable was thermal conductivity of the knitted fabric (Yingngam, 2025). The experimental design variables and levels are shown in Table 1.

Table 1. Factors and levels for screen printing

Factors	Name	Min	Max
A	Viscosity	56 centistokes	62 centistokes
B	Number of strokes	5	10

Two factors and two levels experimental design CCD (central composite design) design generated by design expert with 13 experimental runs with different default random combinations (table 2) was used for development of experimental samples. Samples were developed by the method of screen printing. In table 2, the default design expert design summary is shown (Šolić, Marić, Peko, & Samardžić, 2025).

Table 2. CCD Experimental Run and Response

Std	Run	Factor 1 A: Viscosity Centistokes	Factor 2 B: Number of Strokes Number	Response 1 Thermal Conductivity W/mK
9	1	59	8	0.0411
12	2	59	8	0.043
13	3	59	8	0.041
3	4	56	10	0.0499
4	5	62	10	0.0388
2	6	62	5	0.03
8	7	59	11	0.048
5	8	55	8	0.0495
11	9	59	8	0.041
7	10	59	4	0.036
10	11	59	8	0.041
1	12	56	5	0.04
6	13	63	8	0.034

Results and Discussion

Surface Features of Coated Knitted Fabric

The coated knitted fabric's SEM micrographs show a notable change in surface morphology. The coating layer partially or completely obscures the individual yarns at lower magnification (100 microns) by appearing as a continuous film over the knitted loops (Figure 2). The efficiency of the coating process in altering the textile surface is demonstrated by the comparative SEM study. The coated version of the fabric gives up part of its permeability in return for better surface uniformity and protection, while the uncoated version keeps more flexible and breathable structure. The surface characteristics of created materials were captured using the SEM equipment at the Institution of Excellence, Vignana Bhavana, Manasagongotri, University of Mysore.

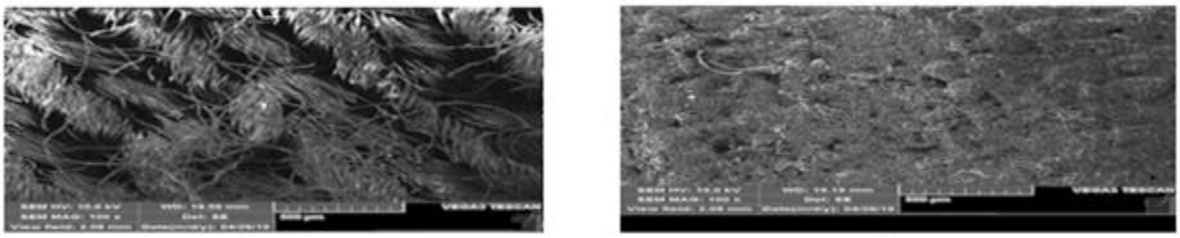

(a) (b)

Figure 2. (a) Surface morphology of knitted fabric uncoated, (b) Surface morphology of coated knitted fabric using kulkote PCM

Thermal Analysis

In order to characterize the thermal phase change of the Kulkote phase change material coated sample, the differential scanning calorimeter (DSC) (SKZ1052B, China) at AASTU (Addis Ababa science and technology university) was used (Figure 3).

Figure 3. Differential scanning calorimeter (DSC) (SKZ1052B, China)

The DSC scanning experiments were carried out in a nitrogen gas atmosphere with a flow rate of 120 mL·min^{-1} and heating rates of 10°C per minute from 25 to 700°C.

Figure 4 represents a thermally stimulated voltage (TSV) measurement, commonly used to investigate charge trapping, dipole relaxation, or phase transitions in materials. Initially, the voltage remains near zero or slightly negative up to around 200 °C, indicating minimal thermally activated processes. Between 200 °C and 400 °C, small fluctuations and a gradual voltage rise suggest the activation of local molecular motions or the release of shallow trapped charges. A sharp and significant voltage peak appears around 450 °C, which is characteristic of a major thermal event such as a phase transformation, decomposition, or the release of deeply trapped charges, depending on the nature of the material. After the peak, the voltage drops rapidly, indicating the completion of the major transition, and then shows a gentle rise beyond 500 °C, possibly due to residual conduction or material degradation. Overall, the material exhibits relatively stable behavior at lower temperatures, with a pronounced transition occurring near 450 °C, marking a critical change in its electrical or structural properties.

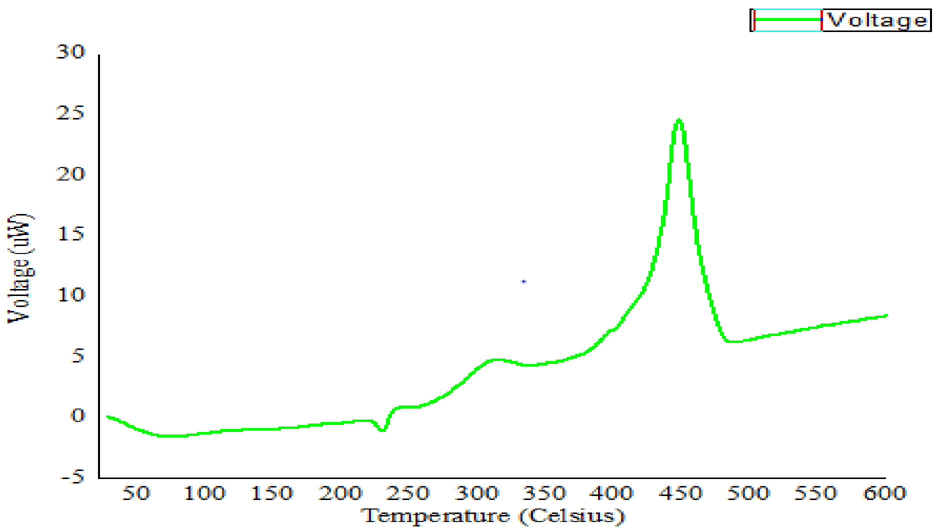

Figure 4. Differential scanning calorimeter – Heating curve- Uncoated

Figure 5 illustrates the variation of voltage (in µV) with temperature (in °C) and reflects the thermally stimulated behavior of the material. Initially, a small negative voltage is observed up to about 50 °C, followed by a generally stable region with minor fluctuations until approximately 200 °C. A noticeable increase in voltage begins around 200 °C, with several small peaks and valleys indicating successive thermal activation of localized relaxation processes or release of shallow trapped charges.

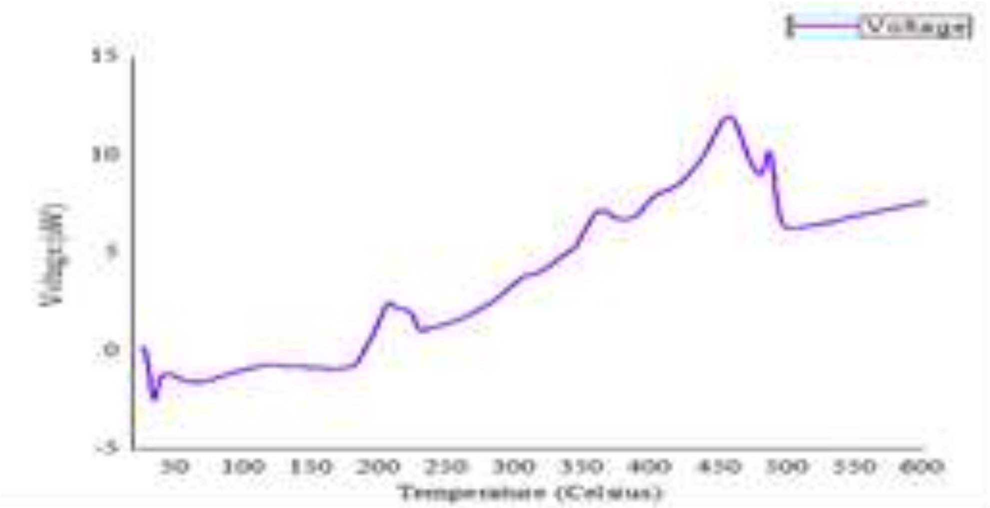

Figure 5 Differential scanning calorimeter – Heating curve- Coated

A prominent peak occurs around 450 °C, suggesting a major event such as a phase transition, decomposition, or the discharge of deeply trapped charges. Following this peak, the voltage decreases sharply but resumes a gradual increase beyond 500 °C, which could be attributed to ongoing conduction or minor degradation processes. Overall, the material shows multiple stages of thermal activation, with the most significant structural or electrical changes occurring near 450 °C.

Fourier Transformer Infrared Spectrometer (FTIR) Analysis

A Fourier transformer infrared spectrometer with attenuation total reflection (FTIR–ATR detector of iS50 smart Germany) was used to characterize the functional group bands in both coated and uncoated samples (Figure 6). With 32 scans and a resolution of 16 cm^{-1}, the middle infrared reflection was set in the 4000–400 cm^{-1} wavenumber absorption bands.

Figure 6. (FTIR–ATR) detector of iS50 smart Germany)

This FTIR spectrum contrasts an uncoated cloth's infrared transmittance with that of a coated fabric (red line) (black line). Materials can be identified by their functional groups and chemical bonds using Fourier Transform Infrared Spectroscopy (FTIR) (Figure 7). Three prominent peaks can be seen at 2915 cm^{-1}, 1729.86 cm^{-1}, and 1159 cm^{-1}. The presence of greater or more concentrated chemical groups is shown by the coated fabric's stronger absorption bands at these locations as compared to the uncoated fabric. The peak at 2915 cm^{-1} usually represents C–H stretching vibrations (from $–CH_2$ or $–CH_3$ groups), C=O stretching (carbonyl groups) is represented by 1729.86 cm^{-1}, and C–O–C or C–O stretching is frequently linked to esters or ether connections.

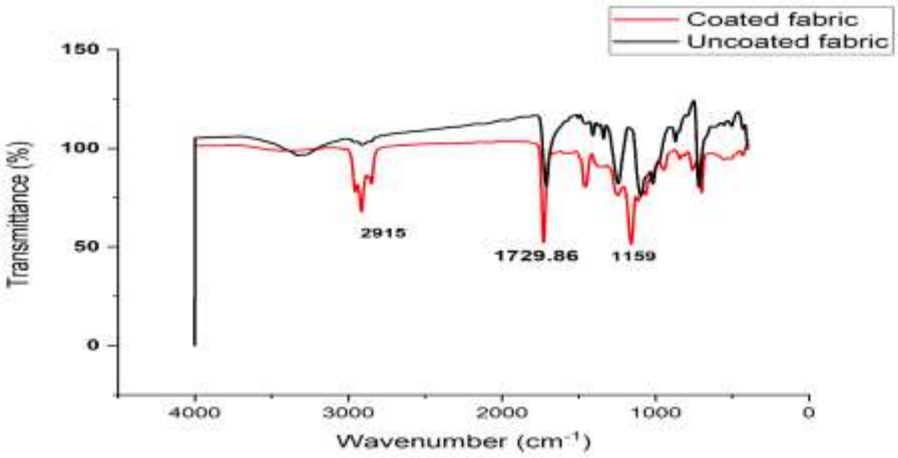

Figure 7. (FTIR–ATR) detector of iS50 smart Germany)

The fabric's chemical coating is the cause of the variations in the FTIR spectra that are seen. The coated sample's increased peaks indicate the presence of additional functional groups, most likely from a polymeric or composite coating made of polyester, polyurethane, or other synthetic or bio-based resins. These coatings can enhance the strength, functionality, and water resistance of fabrics (e.g., flame retardance, antibacterial activity). The spectral alterations verify that the fabric surface has been successfully chemically modified, with the coating adding or intensifying vibrational modes that match particular chemical bonds.

Physical Properties of Uncoated and Coated knitted fabrics

Fabric thickness tester is a specialized equipment to determine the thickness of fabrics. Latest model equipment was employed with modern facilities like modern aesthetics, maximum capacity 10 mm and accuracy 0.01mm and portable and handy to carry anywhere.

Thirteen distinct sample numbers are shown in the table and bar graph (Table 3 and Figure 8), which compares the thickness measurements (in millimeters) of uncoated and coated knitted samples. Although there is considerable variation in thickness between the many samples for the coated and uncoated categories, the general pattern unmistakably shows that the coating on the knitted cloth increased the thickness. The percentage of screen-printed coated fabrics that was added was 69.72.

Table 3. Thickness (mm) value of uncoated and Coated screen-printed samples

Sample no.	Uncoated knitted	Coated knitted
1	0.48	0.55
2	0.47	0.58
3	0.49	0.56
4	0.48	0.55
5	0.48	0.52
6	0.47	0.56
7	0.49	0.56
8	0.48	0.54
9	0.47	0.49
10	0.47	0.56
11	0.48	0.51
12	0.48	0.56
13	0.46	0.51

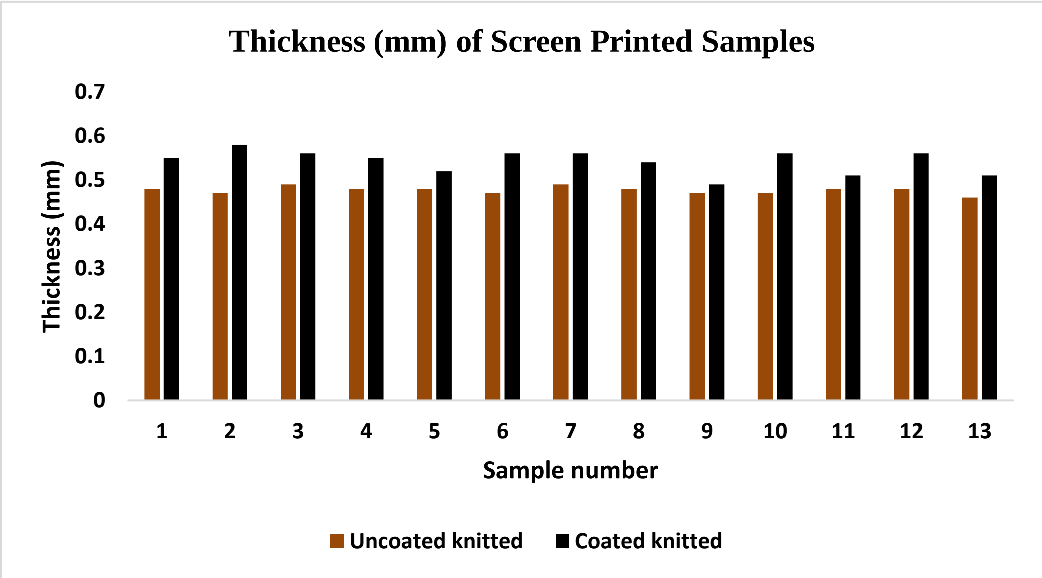

Figure 8. Thickness of Screen-Printed uncoated vs coated samples

Abrasion Test

The ASTM D4966 (abrasion) and ASTM D4970 (pilling) standards were followed when conducting the Martindale Abrasion and Pilling Test (Figure 9) on knitted samples.

The bar graph (Figure 10) shows the degree of pilling, which is a measure of abrasion resistance, for six coated samples and an uncoated sample. A moderate level of abrasion resistance is indicated by the degree of pilling of 4, which is present in both the coated samples 1, 3, 5, and 6, as well as the uncoated sample. With a score of 5, coated samples 2 and 4 exhibit a greater degree of pilling, indicating a marginally lower level of abrasion resistance in comparison to the other samples. (Table 4).

Figure 9. Abrasion testing of screen-printed samples

Table 4. Degree of pilling assessment of screen-printed samples

No.	Degree of pilling
Uncoated	4
1	4
2	5
3	4
4	5
5	4
6	4

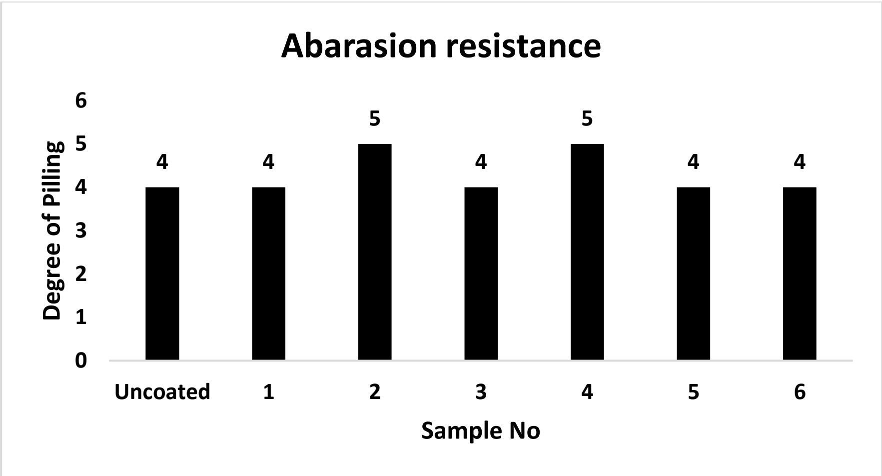

Figure 10. Degree of Pilling of screen-printed samples

Stiffness testing

The ASTM D1388-08 Standard Test Method for Fabric Stiffness is provided. These samples were tested using the Standard Test Method for Stiffness of Fabrics (ASTM D1388-08) by a fabric stiffness tester at the Ethiopian Institute of Textile and Fashion Technology laboratory at Bahir Dar University.

Table 5. Test result of the stiffness bending length (cm) of the samples

Sample no.	Knitted
Uncoated	0.66
1	1.35
2	1.65
3	1.35
4	1.45
5	1.55
6	1.765

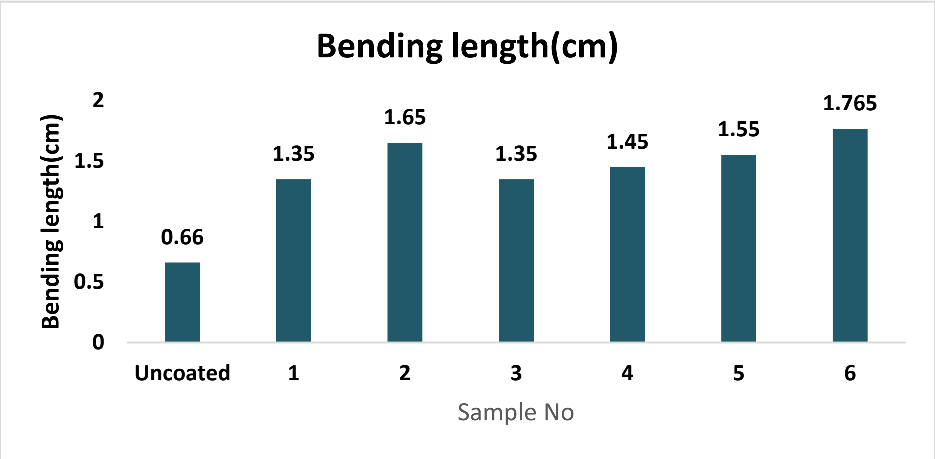

Figure 11. Degree of Pilling of screen-printed samples

The data for knitted samples is shown in Table 5 and Figure 11 above. The first row indicates an "Uncoated" sample with a value of 0.66. Matching values of 1.35, 1.65, 1.35, 1.45, 1.55, and 1.765 are shown in the following rows, which are designated with sample numbers 1 through 6. The coated knitted samples 1 through 6 had values more than twice as high as the uncoated sample and vary somewhat from one another, suggesting that the uncoated knitted sample has a significantly lower value. The coated samples had values ranging from 1.35 to 1.765, indicating that the attribute being tested varies somewhat amongst these coated samples.

A comparison of the fabric weight in grams per square meter (GSM) for each of the thirteen sample numbers shows a similar pattern, as shown in Table 6 and Figure 12 below. The coated knitted samples are consistently heavier than the comparable uncoated knitted samples. It appears that the weight difference between the coated and uncoated versions for each sample is quite uniform, indicating that the weight added to the knitted fabric by the coating procedure is constant.

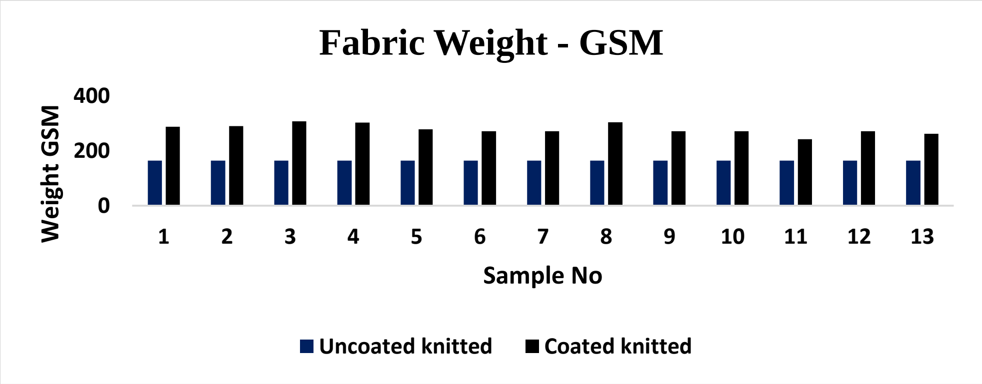

Figure 12. GSM of screen-printed samples

Table 6. GSM (g/m^2) of uncoated and screen-printed samples

Sample no.	Uncoated knitted	Coated knitted
1	164.8	287.6
2	164.7	290.9
3	164.9	307.4
4	164.8	303.7
5	164.8	279
6	164.9	271.6
7	164.8	271.5
8	164.7	304.3
9	164.9	272
10	164.8	271.7
11	164.8	242.8
12	164.7	271.6
13	164.8	262.5

Thermal conductivity test

Lee's disc apparatus was used to ascertain the bad conductor's (Knitted cotton fabrics) coefficient of thermal conductivity. The Lee disc apparatus is made up of a metallic disc that sits above a hollow cylinder (steam chamber) that is 5 cm deep and has the same diameter. There are steam inlet and outlet tubes. It also features radial holes where thermometers can be inserted. A material's capacity to conduct heat is indicated by this. Steam quickly reaches a steady condition as it passes through the cylindrical tank. Heat radiated by the Lees disc is equivalent to the heat carried by the poor conductor in the steady state. The steady-state rate of conduction-based heat transfer (H) is determined by ASTM C-518-15 method.

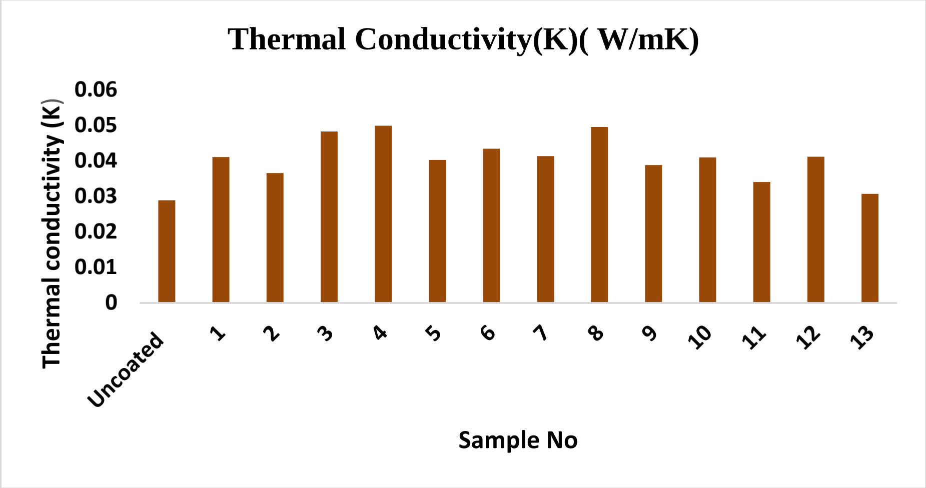

Figure 13. Comparative graph of Thermal Conductivity of PCM uncoated and coated samples

An uncoated sample and thirteen coated samples' thermal conductivity (K), expressed in Watts per meter-Kelvin (W/mK), are shown in the bar graph and Table 7. The sample that is not coated has the lowest thermal conductivity, which is around 0.029 W/mK. The thermal conductivity typically rises with coating in all samples, ranging from around 0.034 W/mK to 0.050 W/mK (Table 7). The coated samples with the highest thermal conductivity values are, notably, samples 3, 4, and 8 (Figure 13). This implies that the coating procedure tends to improve the knitted fabric's thermal conductivity. However, the degree of this improvement varies based on the coated sample in question.

Table 7. Thermal conductivity values for uncoated and screen-printed knitted samples

Sample No	Thermal Conductivity(K)(W/mK)
Uncoated	0.02893
1	0.04101
2	0.03652
3	0.04825
4	0.04987
5	0.04024
6	0.04337
7	0.04133
8	0.04953
9	0.03882
10	0.041
11	0.03404
12	0.0411
13	0.03067

Statistical Data Analysis

Optimizing the fabric coating process with thermal conductivity as the response and viscosity and stroke count as parameters is made possible by using Design Expert® software to perform Central Composite Design (CCD) statistical analysis. All things considered, Design Expert improves the accuracy, effectiveness, and interpretability of CCD-based optimization, which makes it extremely useful for enhancing thermal performance, coating uniformity, and manufacturing efficiency in textile applications (Su, Zhu, Fan, Liu, & Tian, 2025).

Analysis of Variance

An F-value of 104.50 and a p-value of less than 0.0001 in the analysis of variance (ANOVA) results suggest that the model as a whole is statistically significant. This demonstrates how well the model accounts for a significant amount of the response variable's variability. Both Viscosity (A) and Number of Strokes (B), among the parameters taken into consideration, show highly significant impacts on the reaction, with huge F-values of 178.78 and 129.45, respectively, and extremely low p-values (< 0.0001). These results (Table 8) show that both parameters are important; however that viscosity has a somewhat bigger effect according to the F-statistic.

The analysis of variance (ANOVA) results show that the overall model is statistically significant, as indicated by a high F-value of 104.50 and a p-value less than 0.0001. This confirms that the model effectively explains a large portion of the variability in the response variable. Among the factors considered, both Viscosity (A) and Number of Strokes (B) demonstrate highly significant effects on the response, with extremely low p-values (< 0.0001) and large F-values of 178.78 and 129.45, respectively. These findings highlight that both parameters play critical roles, with Viscosity having a slightly greater impact based on the F-statistic (Uçurum, Özdemir, & Teke, 2025).

However, as indicated by its low F-value of 0.3312 and high p-value of 0.5791, the interaction effect between Viscosity and Number of Strokes (AB) is not statistically significant. This implies that each of the two factors functions independently and that their combined influence does not substantially add to the variability in the response variable. Consequently, simulating their interaction does not increase the model's capacity to explain. In summary, the model fits well, and both viscosity and the number of strokes are important factors, but they hardly interact.

Table 8. ANOVA Table for factors and Response for screen-printed knitted samples

Source	Sum of Squares (SS)	Df	Mean Square (MS)	F-value	p-value	Significance
Model	0.0004	3	0.0001	104.5	< 0.0001	Significant
A – Viscosity	0.0002	1	0.0002	178.78	< 0.0001	Highly Significant
B - Number of Strokes	0.0002	1	0.0002	129.45	< 0.0001	Highly Significant
AB (Interaction)	4.162×10^{-7}	1	4.162×10^{-7}	0.3312	0.5791	Not Significant
Residual Error	1.131×10^{-5}	9	1.257×10^{-6}			
Lack of Fit	8.183×10^{-6}	5	1.637×10^{-6}	2.09	0.2471	Not Significant
Pure Error	3.128×10^{-6}	4	7.820×10^{-7}			
Total (Corrected)	0.0004	12				

Main and Interaction Effects of Factors on Thermal Conductivity

Viscosity (A) and stroke count (B) have separate effects on thermal conductivity, as seen in these main effect charts (Figure 14). Viscosity's effect is shown in the left plot while the number of strokes is held constant at a central value of 7.5, and the effect of the number of strokes while viscosity is held constant at its central value is shown in the right plot (59). Each graphic has a y-axis for thermal conductivity and an x-axis for the factor under study (viscosity on the left, number of strokes on the right). The dashed lines in each plot indicate the 95 percent confidence interval around the average trend of thermal conductivity, which is represented by the solid line as the corresponding factor varies. The expected heat conductivity at the midpoints of both variables is shown by the red crosshairs on each plot.

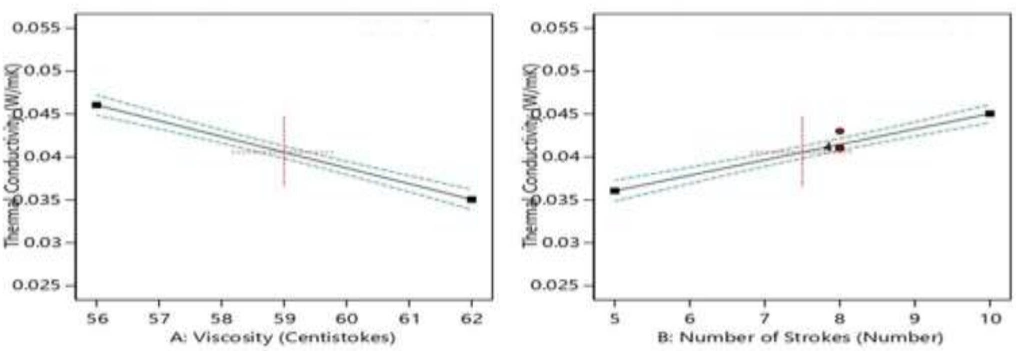

Figure 14. Main Effect plot of factors on Thermal Conductivity

This interaction plot investigates the ways in which viscosity (A) affects thermal conductivity at various stroke counts (B). The y-axis displays the heat conductivity in W/mK, while the x-axis depicts viscosity in centistokes. A lower number of strokes (B = 5) is represented by the black line with square markers, while a larger number of strokes (B = 10) is represented by the red line with triangular markers. These two lines on the plot each reflect a different level of the number of strokes. The intermediate values of the number of strokes (B = 8) are represented by the green circular marks. The 95 percent confidence interval bands, which show the uncertainty in the anticipated thermal conductivity at each viscosity level for the specified number of strokes, are indicated by the dashed lines that surround each main line (Figure 15).

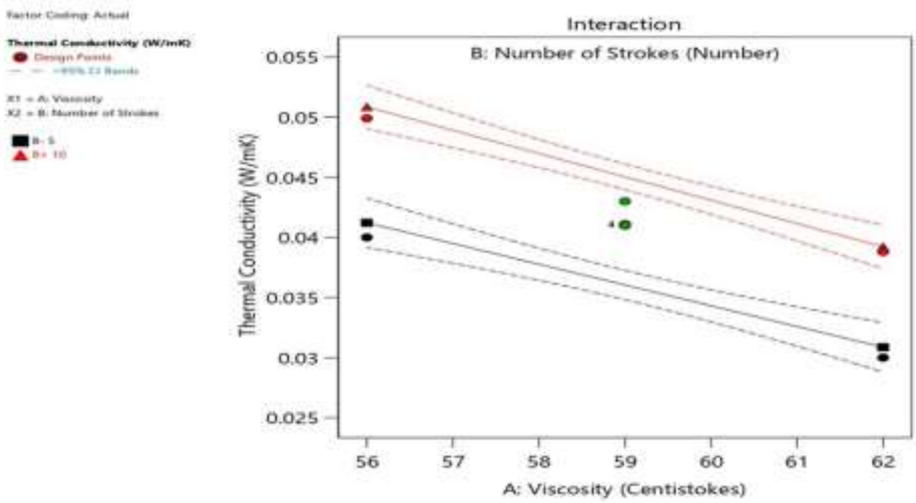

Figure 15. Interaction Effect plot of factors on Thermal Conductivity

An interaction between the two factors that is statistically not significant is indicated by the lines' parallelity. In the absence of interaction, two parallel lines should be visible, showing that viscosity has the same impact on thermal conductivity regardless of the number of strokes. As viscosity rises, the lines diverge, indicating that the number of strokes utilized determines the ideal viscosity for reaching the required thermal conductivity.

2-D contour plot Analysis

This contour plot shows how a material's thermal conductivity is influenced by two variables: the number of strokes (B) and viscosity (A), which is expressed in centistokes. Different levels of thermal conductivity are represented by the colored regions and contour lines; higher thermal conductivity is indicated by warmer colors (orange and red) and lower thermal conductivity by cooler colors (green and blue). The plot illustrates how variations in viscosity and stroke count have an impact on the final thermal conductivity at the same time (Figure 16).

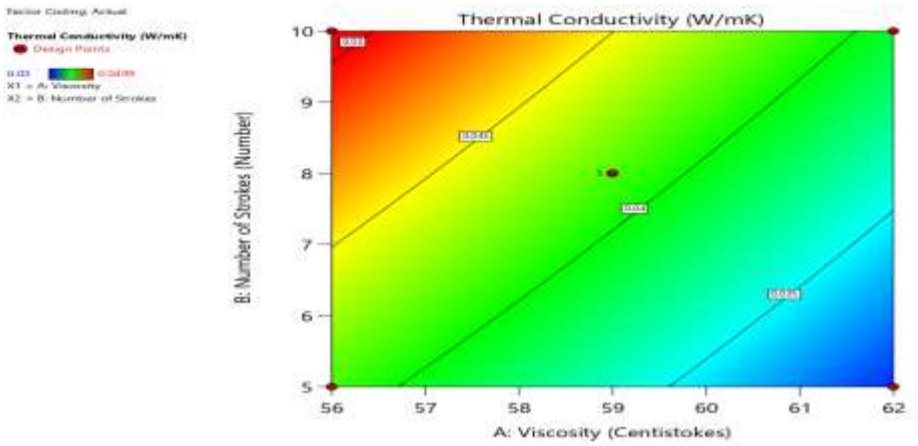

Figure 16. 2D Contour for factors and Thermal Conductivity

The contour plot's color gradient gives the thermal conductivity's magnitude a visual expression. A decrease in thermal conductivity values is indicated by the transition from red to blue. The maximum levels of thermal conductivity seen or anticipated within the investigated range of viscosity and stroke count are shown by the deep red area in the top left corner. A systematic decrease in thermal conductivity is indicated by the colors' progression from orange, yellow, and green to blue in the lower right corner. Therefore, one can immediately determine if the thermal conductivity is relatively high or low by merely seeing the color of a particular spot on the plot. A location located in a primarily green environment, for example, would have a lower thermal conductivity than a point located in a reddish area. These color zones are further defined by the contour lines, which serve as limits between various thermal conductivity levels and enable a more accurate calculation of the thermal conductivity value at any given combination of viscosity and stroke count.

3D Surface Plot Analysis

A broad pattern emerges from surface analysis: heat conductivity tends to decrease with increasing viscosity. At the same time, the thermal conductivity seems to decrease as the number of strokes increases. This is seen by the surface's downward slope as we proceed along the axes of viscosity and stroke count. The surface's curvature—or lack thereof—reveals whether the correlations between the variables and thermal conductivity are linear or non-linear. In this instance, the surface seems to be quite flat, indicating that within the ranges under study, the effects of viscosity and the number of strokes on heat conductivity are essentially linear. These patterns are further supported by the color gradient, which shows that the highest thermal conductivity values are typically seen at lower viscosity and stroke count levels, shifting to lower values as both grow. The degree to which the fitted model accurately captures the observed data is shown by the design points' proximity to the surface (Figure 17).

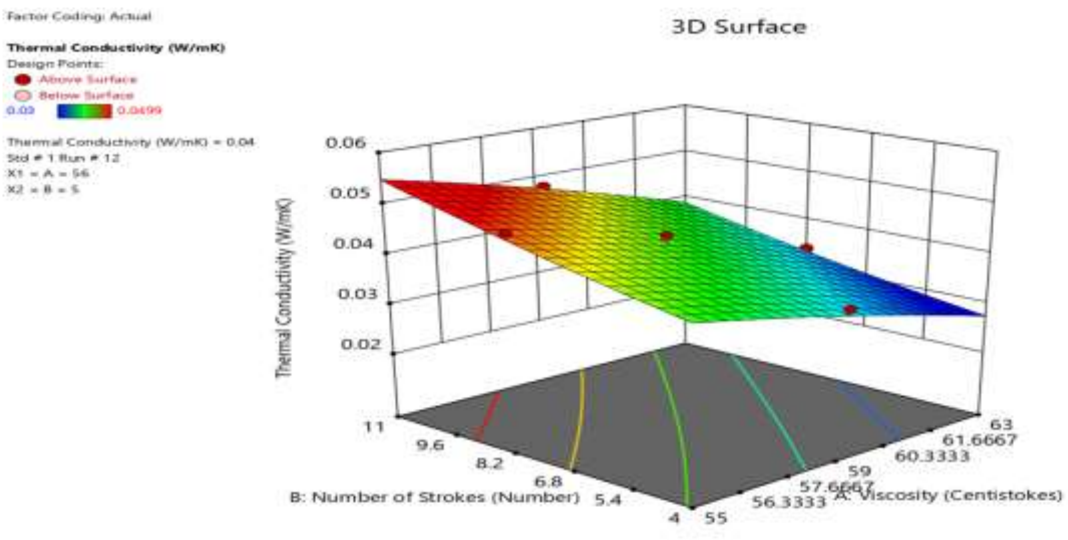

Figure 17. 3D surface plot for factors and Thermal Conductivity

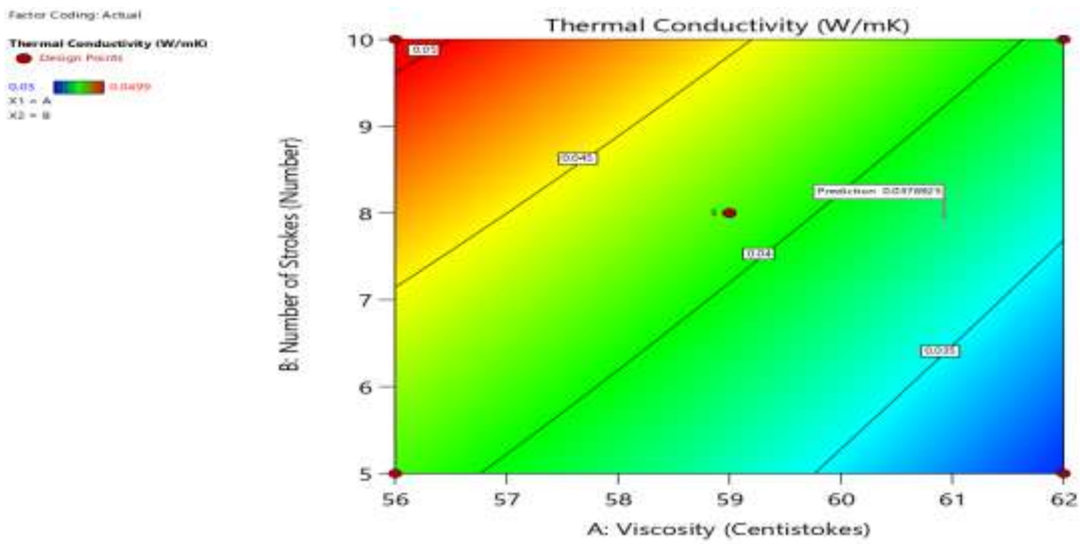

Figure 18. Optimized 2D Contour for factors and Thermal Conductivity

The optimal relationship between viscosity (A), the number of strokes (B), and heat conductivity is graphically shown by the 3D surface plot (Figures 18 & 19). At lower levels of both viscosity and the number of strokes, the region of highest anticipated thermal conductivity is represented by the peak of the surface, which is shown by the warmer hues (towards red). A decrease in heat conductivity is indicated by the surface turning cooler (blue and green) when we increase the viscosity and the number of strokes. This implies that it is best to operate at lower levels of viscosity and stroke count to maximize thermal conductivity within the experimental region under study. This view is further supported by the design points displayed on the surface and projected onto the base, which demonstrate that the area with the lowest viscosity and fewer strokes had the maximum thermal conductivity values.

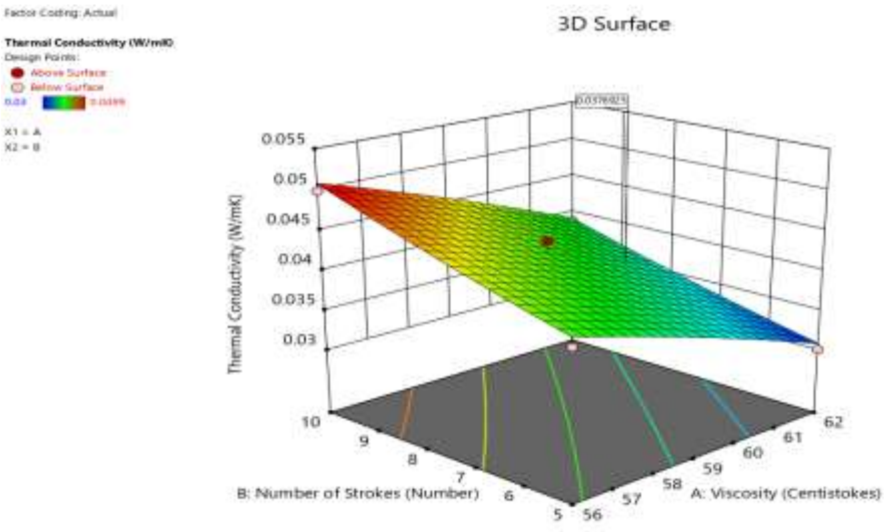

Figure 19. Optimized 3D surface plot for factors and Thermal Conductivity

Conclusions

The influence of viscosity and the number of strokes, two important coating process variables, on the thermal conductivity of cotton knitted fabrics treated with phase change material (PCM), specifically Kulkote, was successfully investigated in this work. Using the Response Surface Methodology framework and a central composite design (CCD), investigate in detail how changes to these parameters affect the functional performance of textiles coated with PCM.

The findings demonstrated that the number of strokes and viscosity have a substantial impact on the treated fabrics' thermal conductivity. Notably, thermal conductivity tended to be improved by lower viscosity values and fewer coating strokes. This is explained by the PCM's improved penetration and even dispersion throughout the fabric structure, which facilitates more effective heat transfer during the phase change process.

Significant variations between uncoated and coated fabrics were found by the SEM morphological examination. Smoother, more compact surfaces with fewer gaps and inter-yarn spaces were seen in the coated samples, which probably enhanced their resilience to environmental factors like moisture and abrasion. These structural alterations highlight how the coating improves both thermal and physical characteristics.

The relevance of both independent variables—viscosity and number of strokes—on the response variable (thermal conductivity) was validated by statistical analysis using ANOVA; however, the interaction effect between the two was not statistically significant.

In conclusion, a viable path toward creating functional textiles with improved thermoregulatory behavior is the incorporation of Kulkote PCM via controlled screen printing. The results provide the textile finishing industry with important new information, especially when it comes to creating smart materials for use in protective gear, sporting, sleeping, and clothes. For wider applicability, future studies could examine the long-term resilience of PCM coatings in practical settings and extend to different textile topologies and PCM kinds.

Acknowledgements

The authors wish to acknowledge the FDRE TVT Institute for giving us the opportunity to carry out this research work.

Declaration of Competing Interest

The authors declare no conflict of interest.

References

Aksoy, S. A., Yılmaz, D., Maleki, H., Rahbar, R. S., & Barani, H. (2024). Fabrication and characterization of nanoencapsulated PCM-doped cotton/PAN nanofiber-based composite yarns for thermoregulation. *Journal of Energy Storage, 101*, 113849. https://doi.org/10.1016/j.est.2024.113849

Cenik, İ., Oktay, B., Nallbani, B. G., & Kayaman-Apohan, N. (2025). Design and evaluation of MOF-containing PCM materials for energy storage in textile applications. *Polymer Engineering & Science, 65*(6), 2944–2954. https://doi.org/10.1002/pen.27190

Chen, J., Yan, Z., Qiao, Y., Lin, F., Wang, Y., & Zhou, H. (2024). Heat dissipation design based on topology optimization and auxiliary materials. *Journal of Electronic Packaging, 146*(2). https://doi.org/10.1115/1.4064099

Ding, W.-T., Liu, Y.-K., Meng, Y., Yang, H., Jiao, X.-Y., Hou, P.-X., & Liu, C. (2025). A single-wall carbon nanotube non-woven fabric–phase change material hybrid for wearable thermal management. *Carbon*, 120027. https://doi.org/10.1016/j.carbon.2025.120027

El Majd, A., Sair, S., Ait Ousaleh, H., Bouhaj, Y., Belouaggadia, N., Younsi, Z., & El Bouari, A. (2024). Advancing tent thermoregulation: Integrating shape-stabilized PCM into fabric design. *Journal of Energy Storage, 95*, 112681. https://doi.org/10.1016/j.est.2024.112681

Kadam, V., Saini, H., Verma, K., Dubey, I., & Verma, P. (2024). Prospects of wool and woolen products. In *The Wool Handbook* (pp. 593–610). Elsevier. https://doi.org/10.1016/B978-0-323-99598-6.00016-5

Lang, X., Xiang, X., & Gao, J. (2024). Preparation and performance of phase change thermoregulating fabric with high heat storage density via spray coating. *Journal of Engineered Fibers and Fabrics, 19*, 15589250241266976. https://doi.org/10.1177/15589250241266976

Li, B., Song, S., Tian, J., Ren, B., Yu, J., & Wang, Y. (2025). Thermal performance of a novel composite phase change material for solar-assisted air source heat pump packed bed thermal energy storage application. *Applied Thermal Engineering, 258*, 124582. https://doi.org/10.1016/j.applthermaleng.2024.124582

Omen, Ł., Panas, A. J., Wajdzik, P., & Szczepaniak, R. (2025). Effect of the addition of microencapsulated phase change material to epoxy resin on the thermal diffusivity of the resulting structure. *Advances in Science and Technology: Research Journal*, *19*(2), 445–452. https://doi.org/10.12913/22998624/196408

Raoux, S. (2009). Phase change materials. *Annual Review of Materials Research*, *39*(1), 25–48. https://doi.org/10.1146/annurev-matsci-082908-145405

Shamsudin, M. A., Mustapha, F., Abdullah, M. N. I., & Mustapha, M. (2025). Sustainable aluminosilicate coatings from palm oil waste for enhanced thermal and microstructure properties. *Materials*, *18*(4), 821. https://doi.org/10.3390/ma18040821

Shuai, Y., Zhang, C., Hu, X., He, S., & Gong, X.-L. (2025). The performance of comprehensive structural parameter for optimization of thermal performance of PCM composite under different heating conditions. *Journal of Energy Storage*, *114*, 115781. https://doi.org/10.1016/j.est.2025.115781

Šolić, T., Marić, D., Peko, I., & Samardžić, I. (2025). Optimization of coating process parameters by analysis of target powder thickness and regression modeling. *Applied Sciences*, *15*(2), 673. https://doi.org/10.3390/app15020673

Su, Y., Zhu, Y., Fan, Y., Liu, S., & Tian, M. (2025). Development of phase-change protective clothing for improving safety of firefighters in low thermal radiation. *International Journal of Occupational Safety and Ergonomics*, 1–9. https://doi.org/10.1080/10803548.2025.2454769

Uçurum, M., Özdemir, A., & Teke, Ç. (2025). Optimization of surface modification parameters of fly ash with high calcium oxide (CaO) content to use as a filling material. *Powder Technology*, *451*, 120463. https://doi.org/10.1016/j.powtec.2024.120463

Yingngam, B. (2025). Design of experiments (DoE) in manufacturing process optimization. In *Sustainable Pharmaceutical Product Development and Optimization Processes: From Eco-Design to Supply Chain Integrity* (pp. 107–139). Springer. https://doi.org/10.1007/978-981-97-9707-3_5